

# Tetragonal-to-monoclinic phase transformation in CeO<sub>2</sub>-stabilized zirconia under multiaxial loading

G. Rauchs<sup>a,1</sup>, T. Fett<sup>b,\*</sup>, D. Munz<sup>a,b</sup>, R. Oberacker<sup>c</sup>

<sup>a</sup>Universität Karlsruhe, Institut für Zuverlässigkeit und Schadenskunde im Maschinenbau, D-76021 Karlsruhe, Germany

<sup>b</sup>Forschungszentrum Karlsruhe, Institut für Materialforschung II, D-76021 Karlsruhe, Germany

<sup>c</sup>Universität Karlsruhe, Institut für Keramik im Maschinenbau - Zentrallabor, D-76128 Karlsruhe, Germany

Received 9 December 1999; accepted 27 April 2000

## Abstract

Critical stresses for the initiation of the tetragonal-to-monoclinic phase transformation in 9Ce-TZP zirconia materials with five different grain sizes have been studied. The influence of the grain size on the critical transformation stresses has been investigated in multiaxial stress states, namely, in four-point bending, biaxial bending and torsion. It was found that phase transformation occurs as a homogeneous phase transformation with a transformation strain increasing continuously with increasing applied stress and also as an autocatalytic phase transformation with the autocatalytic formation of transformation bands normal to the maximum principal stress. An investigation of the critical transformation stresses under different multiaxial loads in the tensile regime, i.e. with positive hydrostatic stress, showed that both the homogeneous and the autocatalytic transformation do not follow the shear-dilatant criterion investigated in multiaxial compressive testing. The experiments showed that under multiaxial loading the onset of both transformation types can be predicted with the maximum principal stress transformation criterion, with the difference between the critical stresses of both transformation mechanisms strongly decreasing with grain size. © 2002 Elsevier Science Ltd. All rights reserved.

**Keywords:** Grain size; Mechanical properties; Phase transformation; TZP; ZrO<sub>2</sub>

## 1. Constitutive laws of the tetragonal-to-monoclinic phase transformation

In technical applications of zirconia ceramics, it seems useful to avoid a macroscopically relevant phase transformation in order to prevent the transformation-induced plastic strains and the related microcracking. This can be achieved using a multiaxial transformation criterion. Another application of the constitutive law is the calculation of transformation zones at crack tips to evaluate the R-curve behaviour. Hence, the ability to predict the onset of the tetragonal-to-monoclinic phase transformation in zirconia ceramics for variable stress states using a multiaxial constitutive law is of major importance.

In a first approach,<sup>1</sup> it was presumed that the volume dilatation was the only parameter of a constitutive law, because the transformation shear strains were considered to be fully reduced by twinning. With the volume dilatation being related to the hydrostatic stress, a hydrostatic transformation criterion was proposed:

$$\sigma_h = \frac{\sigma_{ii}}{3} = \sigma_h^* \quad (1)$$

In a set of compressive tests with a multitude of different multiaxial stress states, it was shown that the shear strains have to be included in the transformation criterion.<sup>2–6</sup> Since the shear strains are related to the von Mises stress, a term including the von Mises stress  $\sigma_V$  was included in the transformation law. According to Ref. 2–4 a shear-dilatant criterion was proposed:

$$\frac{\sigma_h}{\sigma_h^*} + \frac{\sigma_V}{\sigma_V^*} = 1 \quad (2)$$

The influence of multiaxiality on the critical transformation strains can be shown in a  $\sigma_h$ – $\sigma_V$ -diagram or in a  $\sigma_1$ – $\sigma_2$ -diagram. Fig. 1(a) and (b) shows the shear-dilatant criterion together with experimental results in such diagrams according to Ref. 2–4 and, Ref. 7 respectively. In Fig. 1a, the von Mises stress  $\sigma_V$  is replaced by an equivalent shear stress  $\tau$  which is proportional to  $\sigma_V$  for the tests in.<sup>4</sup> Both figures represent two different Ce-TZP materials. The phenomenological transformation criterion [Eq. (2)] has been given a theoretical justification in.<sup>8</sup>

\* Corresponding author. Fax: +49-7247-82-2347.

E-mail address: theo.fett@imf.fzk.de (T. Fett).

<sup>1</sup> Now at Materials Science Centre, University of Manchester, UK.

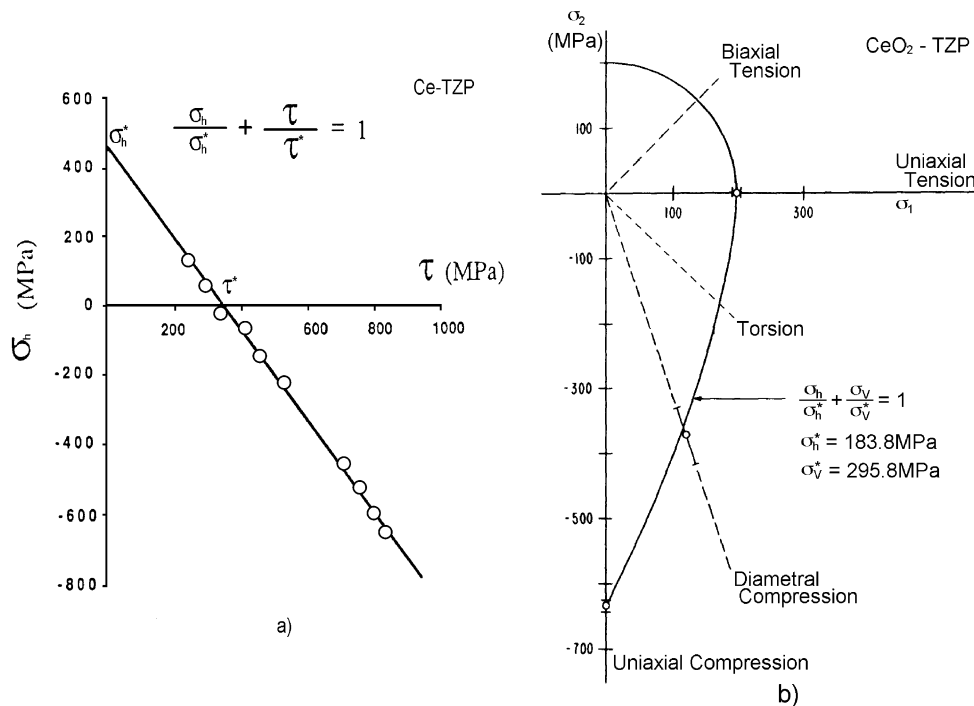


Fig. 1. Shear-dilatant criterion with experimental results: (a)  $\sigma_h$ - $\tau$ -diagram,<sup>4</sup> (b)  $\sigma_1$ - $\sigma_2$ -diagram.<sup>7</sup>

Constitutive laws relying on the von Mises stress only have been used in calculations and theoretical considerations.<sup>9,10</sup> All these transformation criteria are based on critical stresses. Another possibility for deriving a constitutive law is to use the energy balance. This approach is well suited for partially stabilized zirconia, where a regular structure of identical tetragonal inclusions is embedded into the inert cubic matrix.<sup>11</sup>

In fact, the orientation of these ellipsoidal inclusions is dictated by the directions of the cubic lattice structure. This way, the strain field of the bulk material can be derived by averaging the mechanical behaviour of the inclusions over the range of a constitutive element.<sup>12</sup> The strain field of a transformed inclusion has been evaluated in Ref. 13–15 as has the influence of its geometry on crack tip shielding.<sup>16</sup> The influence of microcracking on the constitutive law has been analysed by averaging the effects of particle and microcrack orientation over a constitutive element.<sup>17,18</sup>

In TZP ceramics, however, the orientation and the size of the tetragonal grains follow a random distribution which involves that their interaction is much more complex.

## 2. Experimental

### 2.1. Materials

Five 9 mol% Ce-TZP materials with different grain sizes were investigated.<sup>19</sup> The test materials were pre-

pared from a batch of CeO<sub>2</sub>-ZrO<sub>2</sub> powder (Unitec PCE 14.0-002s). After die pressing at 10 MPa, the plates were isostatically pressed at 200 MPa. The green plates were sintered in air at variable temperatures ranging from 1400 to 1600 °C, with heating and cooling rates of 3 °C/min. In Table 1 the different material data denoted as CeI to CeV are given.

### 2.2. Mechanical experiments

In order to evaluate a multiaxial transformation criterion, three different stress states have been realised in experiments under monotonously increasing load. The stress states have a positive multiaxiality ratio  $\sigma_h/\sigma_v$  in order to achieve multiaxial tensile loads. The experiments were conducted on a load frame equipped with different testing devices to achieve the three stress states:

- Uniaxial tension in four-point bending (4PB) with a specimen geometry of 4×3×48 mm<sup>3</sup> and roller spacings of 40 and 20 mm.
- Biaxial bending (ring-on-ring) with ceramic disks  $\phi$  45×3 mm<sup>3</sup> and load ring diameters of 32 and 16 mm.
- Torsion with ceramic plates with a geometry of 20×3×50 mm<sup>3</sup> leading to shear stresses. The two principal stresses,  $\sigma_1$  and  $\sigma_2$ , are identical with different signs.

The device for torsion testing shown in Fig. 2 was used. Rectangular torsion specimens have been chosen to enable a microscopic examination of a polished surface

Table 1  
Properties of the five materials ( $c_{m,0}$  = initial monoclinic phase content)

Material	Sintering (°C)	Grain size ( $\mu\text{m}$ )	Young's modulus (GPa)	Density (%)	$c_{m,0}$ (%)
CeI	1400	0.9	188	97.6	6.2
CeII	1450	1.4	197	99.9	2.0
CeIII	1500	1.7	199	99.9	2.1
CeIV	1550	2.1	198	99.8	2.1
CeV	1600	2.5	197	99.6	1.9

after testing. The specimens were fixed in cylindrical specimen holders with epoxy resin. The torsion moment was applied by an eccentric load, linked to the specimen through a bending moment-free cardan coupling.

During testing, the following parameters have been recorded:

- the load  $F$  with a load cell to assess the applied stress;
- the local strain at the location of the maximum stress with strain gauges. On some four-point bending specimens, the longitudinal and transverse strains have been recorded;
- the acoustic emission using a piezoelectric device with a resonance frequency of 150 kHz and a low-pass filter of 100 kHz. The device was fixed on the load frame or the specimen holders. The coupling of the measuring device to the structure was achieved by applying silicon glue. The acoustic emission signal enabled the monitoring of the formation of autocatalytic transformation bands;
- after mechanical testing, the monoclinic phase content was investigated on a macroscopic scale using XRD and on a microscopic scale using Raman spectroscopy.

### 2.3. Investigation of the critical transformation stresses

The applied stresses for the ring-on-ring tests were calculated from

$$\sigma = \frac{3F}{4\pi h^2} \left[ (1 - \nu) \frac{D^2 - d^2}{d_a^2} - 2(1 + \nu) \ln \frac{d}{D} \right], \quad (3)$$

where  $D$  and  $d$  are the diameters of the outer and inner loading ring,  $d_a$  is the disk diameter and  $h$  is the thickness of the disk.

For the torsion tests the first principal stress is

$$\sigma = \frac{Fs}{Abh^2}, \quad (4)$$

with  $A = 0.3$ ,<sup>20</sup> specimen width  $h$  and thickness  $b$ . For the torsion moment  $F_s$ , see Fig. 2.

Due to the rectangular shape of the torsion specimens, the torsion shear stresses were superposed by tensile/compressive stresses at the edges. Boundary element calculations<sup>21</sup> showed that these stresses vanish at the centre of the specimen surface, allowing the use of Eq. (4) to compute the shear stresses at this location which exhibits the maximum shear stresses. The direction of the principal stresses was unchanged at the centre of the specimen as well.

The slope of the linear-elastic part of the stress–strain curves was determined by linear regression. The combination of the stress–strain curves with the acoustic emission signal provided the possibility to monitor the onset of phase transformation with two different methods:

- At the intersection of the stress–strain curve with a line parallel to the elastic load line, shifted 5 ppm to the right, the onset of plastic deformation could be monitored. The stress at the intersection point provides the critical stress  $\sigma_c$ .

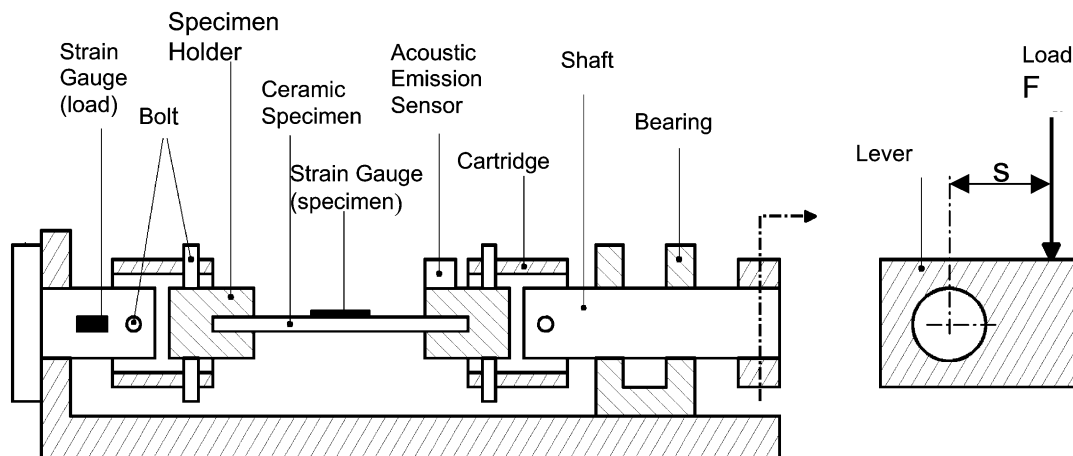


Fig. 2. Device for torsion experiments.

- The onset of autocatalytic transformation band formation, producing audible noise and strong acoustic emission signals at the critical stress  $\sigma_{AE}$ .

### 3. Results

#### 3.1. Critical transformation stresses under multiaxial stress states

In Table 2, the experimentally determined critical stresses for the onset of phase transformation,  $\sigma_c$  and  $\sigma_{AE}$ , are given. In torsion experiments, acoustic emission signals have been recorded during the whole load application. These signals are attributed to friction and have not been used in further evaluations. Therefore, n.m. (not measurable) has been entered into Table 2. In material CeI, no autocatalytic transformation band formation was found. For the other materials, the critical stresses  $\sigma_c$  and  $\sigma_{AE}$  are different, with the difference decreasing for larger grain sizes. This leads to the conclusion that two different transformation mechanisms are occurring in Ce-TZP: A homogeneous phase transformation characterised by  $\sigma_c$  and an autocatalytic phase transformation characterised by  $\sigma_{AE}$ .<sup>19,21</sup> For all three loading modes, the same trend in the increase of the critical stress for homogeneous transformation and in the decrease of autocatalytic transformation with increasing grain size was observed.

From the critical stresses of the homogeneous and the autocatalytic phase transformation, equivalent stresses and other characteristic stresses have been calculated for the three investigated stress states in order to determine a constitutive law for the tetragonal-to-monoclinic phase transformation.

The phase transformation sets in at different hydrostatic stresses. In torsion experiments, with  $\sigma_h = 0$ , phase transformation was found. For these reasons, the hydrostatic transformation criterion has to be rejected as a valid transformation criterion.

The critical transformation stresses measured for homogeneous (Fig. 3a) and autocatalytic phase transformation (Fig. 3b) are shown in a transformation diagram according to Refs. 2–4. The critical hydrostatic

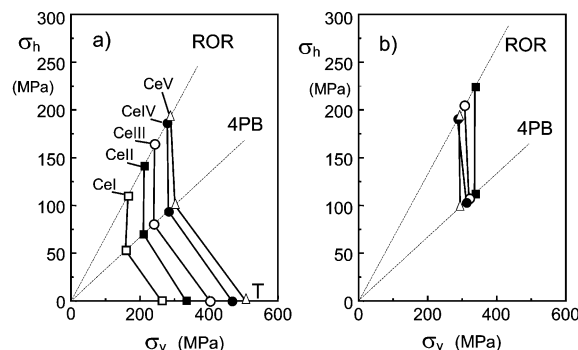


Fig. 3.  $\sigma_h$ - $\sigma_v$ -Diagram according to Refs. 2–4 with shear-dilatant criterion<sup>2–4</sup> for (a) homogeneous and (b) autocatalytic phase transformation (T = torsion test).

transformation stress  $\sigma_h$  is represented over the critical von Mises stress  $\sigma_v$ . It becomes obvious from Fig. 3a that the homogeneous phase transformation sets in at different equivalent stresses, ruling out a von Mises stress criterion for the homogeneous phase transformation. The onset of the autocatalytic phase transformation could be predicted by this criterion. For the homogeneous transformation as well as for the autocatalytic phase transformation, the data of the three stress states cannot be described by a straight line defined by Eq. (2). This shows that the shear-dilatant criterion investigated in compression<sup>2–6</sup> does not remain valid for stress states in the tensile regime, i.e.  $\sigma_h > 0$ .

Fig. 4(a) and (b) shows the measured data for both transformation types in a multiaxial transformation diagram according to Ref. 7. It is easily pointed out that the phase transformation in all of the three stress states sets in at an identical maximum principal stress  $\sigma_1^*$ . This means that the beginning of both the homogeneous and the autocatalytic phase transformation under multiaxial load can be predicted by a maximum principal stress criterion. The condition for the onset of homogeneous phase transformation is

$$\sigma_1 = \sigma_{1,c}^* \quad (5)$$

whereas for the autocatalytic phase transformation it is

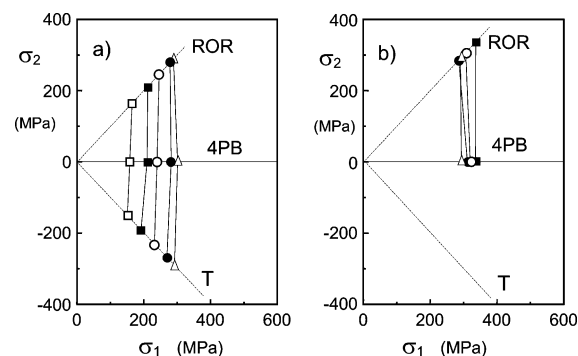


Fig. 4. Multiaxial transformation diagram according to Ref. 7 for (a) homogeneous and (b) autocatalytic phase transformation.

Table 2

Critical transformation stresses (4PB = four-point bending, ROR = ring-on-ring test, n.m. = not measurable)

Material	Grain size ( $\mu\text{m}$ )	$\sigma_c$ (MPa)			$\sigma_{AE}$ (MPa)		
		4PB	ROR	Torsion	4 PB	ROR	Torsion
CeI	0.9	158	165	151	—	—	n.m.
CeII	1.4	210	212	192	336	337	n.m.
CeIII	1.7	240	246	232	320	307	n.m.
CeIV	2.4	282	279	269	312	286	n.m.
CeV	2.5	301	289	292	294	291	n.m.

$$\sigma_1 = \sigma_{1,AE}^* \quad (6)$$

Fig. 5 shows the average values of the critical normal stresses of all three stress states over the grain size for both transformation types. The critical stresses of the homogeneous transformation are lower than those of the autocatalytic phase transformation. The difference between the critical stresses of both transformation types strongly decreases with increasing grain size. For CeV with a grain size of 2.5  $\mu\text{m}$ , the critical stresses are nearly the same.

### 3.2. Autocatalytic transformation structures

On the specimen surfaces of the materials CeII–CeV, a large number of autocatalytic transformation bands

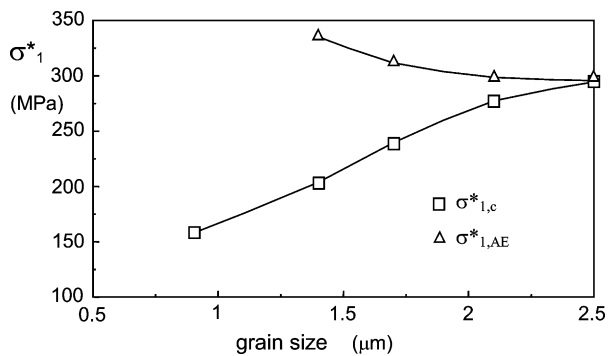
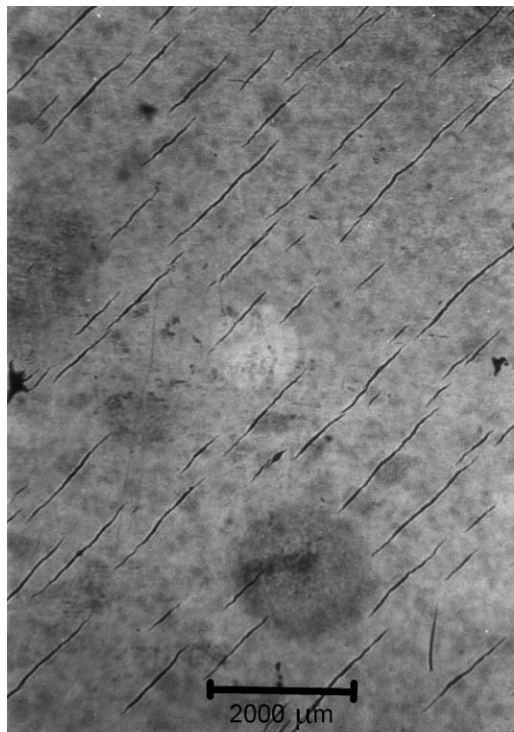


Fig. 5. Influence of the grain size on the critical principal stress for homogeneous and autocatalytic phase transformation.<sup>21,22</sup>

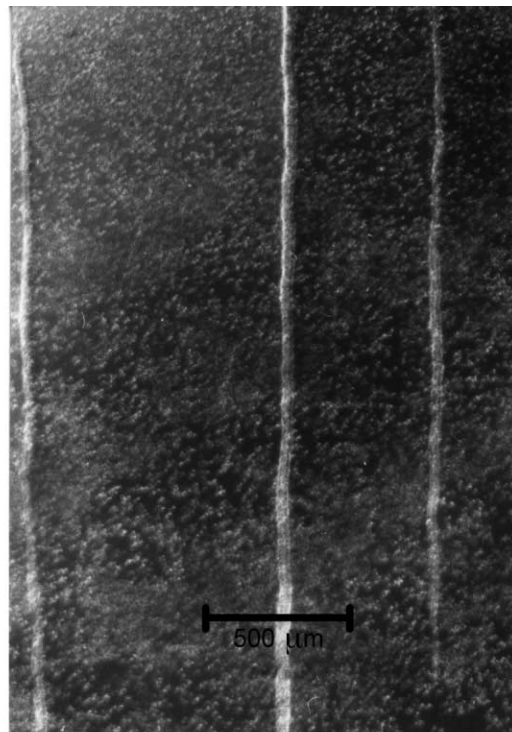
are forming during loading. Microscopic pictures of transformation bands are shown for torsion (Fig. 6a) and for the tensile sides of uniaxial (Fig. 6b) and biaxial bending (Fig. 7) tests. In Figs. 6a and 7, the transformation bands are made visible by defocussing, whereas in Fig. 6b Nomarski-interference was used.

The transformation bands have a variable width between 20 and 100  $\mu\text{m}$  and are irregularly spaced. In uniaxial bending and in torsion, the transformation bands are oriented parallel to each other. On the torsion specimens, the bands are oriented at an angle of 45° towards the torsion axis. In uniaxial bending, they are stretching in the transversal direction of the specimens. On the biaxial bending disks, the transformation bands are pointing in radial direction in the inhomogeneously loaded region, whereas in the biaxially loaded central region, the orientation of the bands is random, thus leading to a net-like structure. From the orientation of the bands under different stress states, it can be concluded that the transformation bands are oriented normal to the direction of the maximum principal stress.

A critical external stress is needed for the formation of autocatalytic transformation bands. At low stress levels, the formation and propagation of transformation bands is inhibited at the edge of torsion and of the biaxial bending specimen. The length of the transformation bands does not depend on the applied stress. The individual transformation bands do not stretch over the total maximally stressed region. This fact has



(a)



(b)

Fig. 6. Autocatalytic transformation bands: (a) torsion specimen (CeIII), (b) tensile surface of a four-point bending specimen (CeII).

also been observed on the larger torsion and biaxial bending specimen as well as on the smaller four-point bending specimen, where the length of some bands was smaller than the specimen width (Fig. 7b). The extremities of the transformation bands are not related to the external stress. Together with the random location of the transformation bands, it seems likely that the locations of starting and ending band formation, i.e. the extremities of the bands, result from microstructural effects with a random distribution.

On bending surfaces under compressive loads, no autocatalytic transformation bands have been found, which leads to the conclusion that in the investigated stress range autocatalytic transformation occurs under multiaxial tensile loads only.

### 3.3. Stress dependence of the monoclinic phase content

During Raman-spectroscopic line scans over the specimens, no increase of the monoclinic phase content was found in CeII–CeV. In these materials, the monoclinic phase is localised in transformation bands. The small amount of monoclinic phase outside of the transformation bands, caused by homogeneous phase transformation, lies below the resolution limit of Raman spectroscopy, thus making it impossible to detect any significant variation of the monoclinic phase content with the applied stress. In case of CeI, a locally varying monoclinic phase content, shown in Fig. 8, was found. In this case, the monoclinic

phase content depends on the applied stress, with the maximum monoclinic concentration being reached at the maximally stressed specimen centre and decreasing towards the unstressed region of the specimen.

On four-point bending specimens and torsion specimens, the strong scattering of the measured monoclinic concentration denies a statement about the influence of the stresses on the monoclinic content. This scattering occurs because of the arbitrary choice of a spectrum background noise, which strongly affects the calculation of the monoclinic phase content in CeI due to the weak monoclinic peaks.

## 4. Discussion

In<sup>2–6</sup> a constitutive law has been derived from experiments with a variable stress state in compression. This transformation law is based on the hydrostatic and von Mises stresses and has been described by Eq. (2). In the compressive experiments, a large number of three-dimensional stress states has been achieved. Due to the symmetry of the specimen and the homogeneous stress field applied, the plastic strains as well as related effects like microcracking could be investigated. In the present investigation, the transformation behaviour under tensile loads, i.e. at the location of positive hydrostatic stresses in the transformation diagram according to Refs. 2–4, has been examined. In this case, a specific testing device had

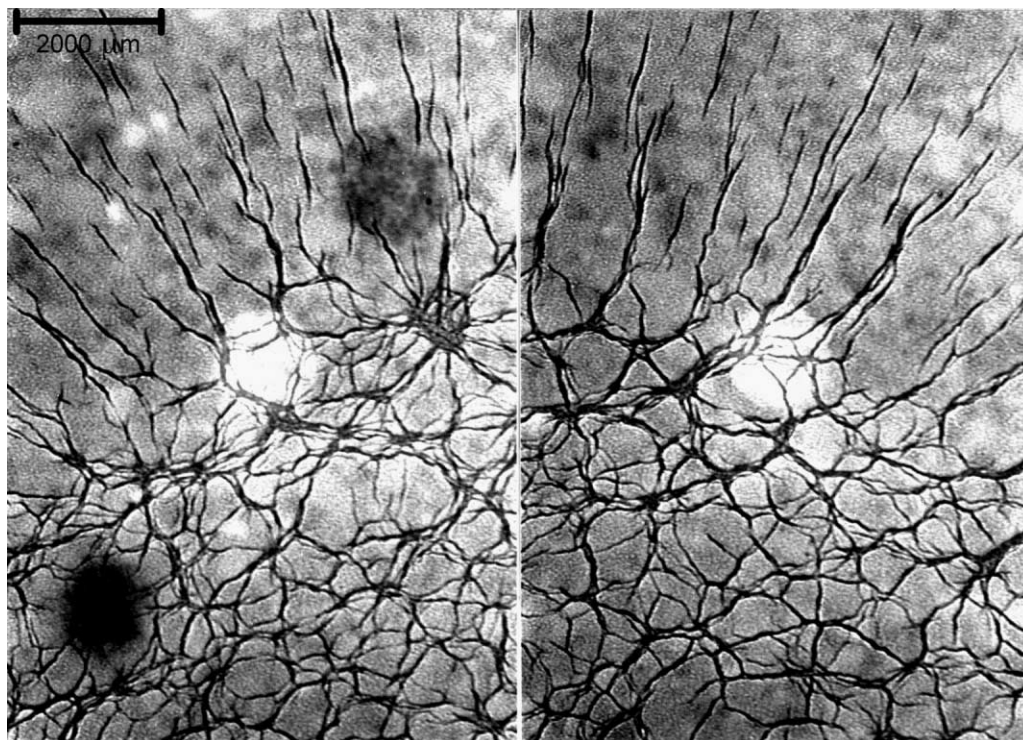


Fig. 7. Autocatalytic transformation bands on a biaxial bending specimen at the boundary of the homogeneous, biaxial and the inhomogeneous, non-biaxial regions on the inner load ring (CeIII).

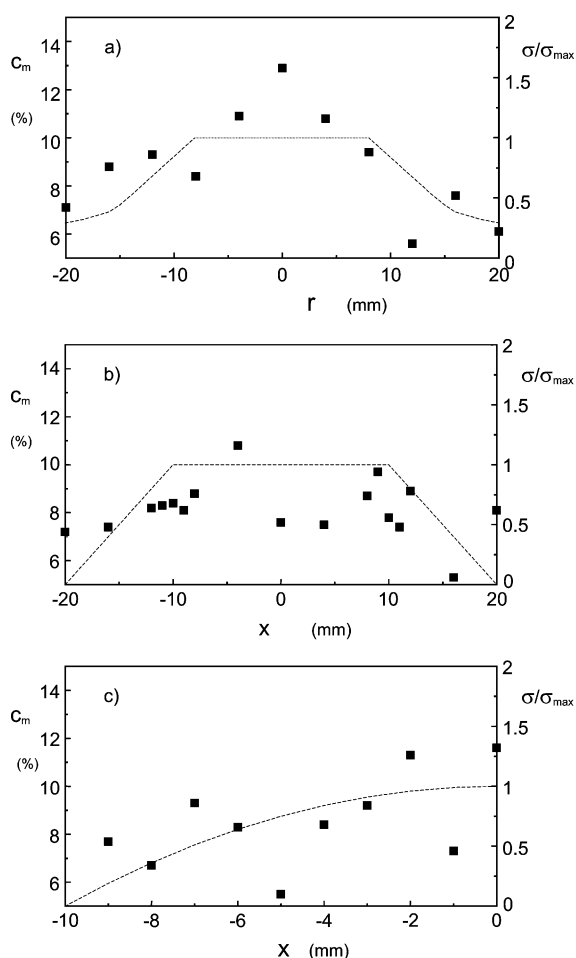


Fig. 8. Monoclinic phase content (a) along the diameter of a biaxial bending specimen (CeI), (b) along the length axis of a four-point bending test specimen and (c) over the half width of a torsion specimen; dotted lines: relative stresses.

to be used for each stress state examined. Using four-point bending, biaxial bending and torsion, three stress states with uniaxial and biaxial tension as well as a torsion stress state could be achieved. These testing geometries exhibit an inhomogeneous stress field. Additionally, the transformation behaviour at the specimen surface can be monitored in these experiments. Due to the free surface, these stress fields are two-dimensional. This also applies to the strain measurements which take place at the specimen surface and, therefore, no information about the out-of-plane strains and the volume dilatation has been obtained. In tensile experiments, a homogeneous tensile stress field can be achieved, yielding the possibility of recording the total strain tensor. Due to the difficulties involved in tensile testing of ceramic materials and considering the fact that the problems encountered remain unchanged for the two other stress states, four-point bending which is easier to perform has been used instead of pure tension. This choice was backed by the fact that the onset of phase transformation can be monitored in an inhomogeneous stress field as well.

In Section 3, the critical phase transformation stresses have been presented for the three stress states mentioned before. For the homogeneous and autocatalytic phase transformation, the critical normal stresses are different. The difference between the two critical stresses decreases with increasing grain size. By representing the experimental data in a transformation diagram according to Ref. 2–4 in Fig. 3, it was shown that the data points do not fit the transformation law described by Eq. (2). This was found for both the homogeneous and the autocatalytic phase transformation. It has to be concluded that the shear-dilatant transformation criterion from<sup>2–4</sup> is not valid for the stress states examined. This is in contradiction to results from<sup>4</sup> shown in Fig. 1a, where the data obtained for positive hydrostatic stresses could be fitted by Eq. (2). In Ref. 2, data obtained from multiaxial compression and from four-point bending in Ce-TZP have been shown in a  $\sigma_h$ - $\sigma_v$ -diagram, with the data point from four-point bending lying below the transformation line described by Eq. (2).

Fig. 4(a) and (b) shows that the data points can be fitted using the criterion of the maximum normal stress. Comparing the results from compression<sup>2–4</sup> with the results for tensile stress states in this investigation, it can be concluded that in the compressive and the tensile regime different transformation laws have to be used.

This raises the question regarding the mechanisms triggering the phase transformation. In the shear-dilatant criterion from<sup>2–4</sup> it is thought that a combination of shear and volume compression of the tetragonal matrix leads to a deformation triggering the transformation of the tetragonal to the monoclinic phase. For loads in the tensile regime, this mechanism does not seem to be valid. With the normal stress criterion, it has to be presumed that local stress concentrators are responsible for the onset of phase transformation. This hypothesis is supported by the fact that location, width and length of the autocatalytic transformation bands scatter strongly. Local stress concentrators are located at microcracks, pores, inclusions, agglomerates and grain boundaries. Microcracks and pores have to be considered the cause of phase transformation during loads with a positive hydrostatic stress, since these flaws remain inactive during compression. Local inhomogeneities in terms of grain size and orientation are supposed to lead to stress concentrations as well. It was found that the individual transformation bands do not stretch over the whole specimen region where the applied stress is superior to the critical stress. The orientation of the transformation bands was found to depend on the external stress field: The transformation bands are oriented normal to the maximum principal stress. This experimental fact could be reproduced during calculations of the transformation zone in a loaded specimen, starting from a transforming circular inclusion.<sup>21</sup> It can be concluded that the size and the location of transformation bands depend on microstructural

parameters. For the onset of autocatalytic phase transformation, a critical external stress is required, with the orientation of the transformation bands being related to the principal directions of the stress field, whereas the monoclinic content depends on the grain size only.

Figs. 9 and 10 show the two different transformation criteria for loads with negative and positive hydrostatic stresses for the homogeneous phase transformation in CeI. For the shear-dilatant criterion, the parameter  $\sigma_V^*$  was taken from the torsion experiments, whereas the free parameter  $\sigma_h^*$  was deduced by a least squares fit through the three data points, since no compressive experiments have been conducted in this investigation to determine this parameter experimentally. Fig. 10 shows the two transformation criteria in a  $\sigma_h$ - $\sigma_V$ -diagram according to<sup>2–4</sup> In that diagram, the curve of the maximum principal stress criterion has been calculated for plane stress, which corresponds to the experimental stress states.

It was found that the onset of the homogeneous phase transformation depends on the maximum normal stress as well. It has to be assumed that similarly to the autocatalytic transformation the homogeneous phase transformation is caused by local stress concentrators. From the investigation of the monoclinic phase content for homogeneous phase transformation, it can be con-

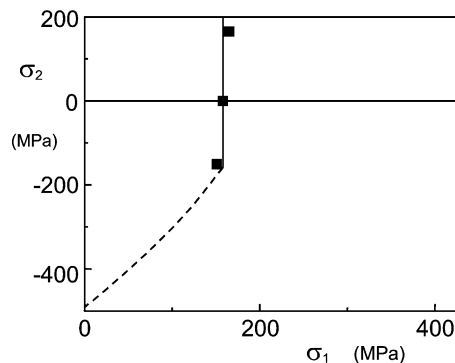


Fig. 9. Multiaxial transformation diagram with the normal stress criterion in the tensile regime (full) and shear-dilatant criterion in the compressive regime (dashed) based on experimental data of the homogeneous transformation in CeI.

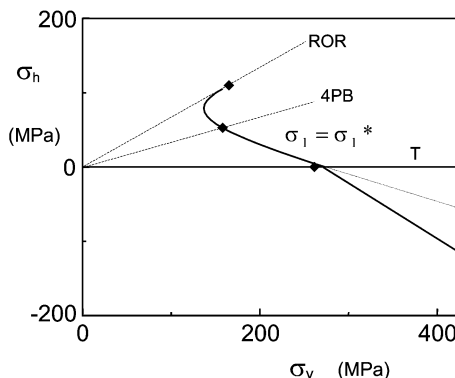


Fig. 10.  $\sigma_h$ - $\sigma_V$ -Diagram according to Ref. 2–4.

cluded that the monoclinic phase content is distributed in a macroscopically homogeneous pattern over the specimen. This implies that the stress concentrators triggering the phase concentration have to be distributed in the specimen in a macroscopically homogeneous way as well. From this point of view, it must be assumed that the homogeneous phase transformation is triggered by stress concentrations on the level of grains or grain boundaries. In the materials with a higher average grain size, these effects strongly decrease. This yields that the homogeneous phase transformation can only be attributed to a small extent to the transformation behaviour in these materials.

## 5. Conclusions

For the investigation of the critical stresses for the initiation of the tetragonal-to-monoclinic phase transformation in 9Ce-TZP zirconia, materials with five different grain sizes have been produced. Taking into account the different grain sizes, the influence of the grain size on the critical transformation stresses has been monitored. The effect of multiaxial stress states on the critical transformation stresses has been investigated in four-point bending, biaxial bending and torsion.

It was found that phase transformation occurs as two different transformation types:

- A homogeneous phase transformation with a transformation strain increasing continuously with increasing stress applied. This transformation type produces the initial deviation from the linear-elastic material behaviour in the stress strain curves.
- An autocatalytic phase transformation, with the autocatalytic formation of transformation bands leading to a strongly inhomogeneous, localised distribution of the monoclinic phase. The transformation bands are oriented normal to the maximum principal stress of the applied stress field. Their location and size vary randomly. The formation of the transformation bands has been monitored by acoustic emission recording.

The grain size influences both types of phase transformation. The critical stresses of the homogeneous transformation increase with increasing grain size. The amount of homogeneous transformation strains decreases strongly with increasing grain size, leading to a strong decrease of the significance of homogeneous transformation to the overall transformation behaviour with increasing grain size. The critical stresses of the autocatalytic phase transformation show a slight decrease with increasing grain size. In the material with the smallest grain size, no autocatalytic phase transformation was found. A similar transformation behaviour



was found in cooling experiments, thus confirming the results of the mechanical experiments.<sup>19</sup>

An investigation of the critical transformation stresses under different multiaxial loads in the tensile regime, i.e. with a positive hydrostatic stress, showed that both the homogeneous and autocatalytic transformation do not follow the shear-dilatant criterion investigated in multiaxial compressive testing. The experiments showed that under multiaxial loading, the onset of both transformation types can be predicted with the maximum principal stress criterion. This discrepancy leads to the conclusion that different mechanisms are responsible for triggering the phase transformation in tensile and compressive stress states. Whereas in compression, a combination of shear and volume strains leads to phase transformation, stress concentrations at microscopic inhomogeneities and flaws, which remain inactive in compression, trigger the phase transformation in tensile stress states. The critical normal stresses of the homogeneous phase transformation are lower than those of the autocatalytic transformation, with the difference strongly decreasing with grain size.

## Acknowledgements

This work was supported by the Deutsche Forschungsgemeinschaft (DFG).

## References

- McMeeking, R. M. and Evans, A. G., Mechanics of transformation-toughening in brittle materials. *J. Am. Ceram. Soc.*, 1982, **65**, 242–246.
- Chen, I. W. and Reyes-Morel, P. E., Implication of transformation plasticity in ZrO<sub>2</sub>-containing ceramics: I. Shear and dilatation effects. *J. Am. Ceram. Soc.*, 1986, **69**, 181–189.
- Chen, I. W. and Reyes-Morel, P. E., Transformation plasticity and transformation toughening in Mg-PSZ and Ce-TZP. *Mat. Res. Soc. Symp. Proc.*, 1987, **78**.
- Chen, W., Model of transformation toughening in brittle material. *J. Am. Ceram. Soc.*, 1991, **74**, 2564–2572.
- Reyes-Morel, P. E., Cherng, J.-S. and Chen, I.-W., Transformation plasticity of CeO<sub>2</sub>-stabilized tetragonal zirconia polycrystals: I. Stress assistance and autocatalysis. *J. Am. Ceram. Soc.*, 1988, **71**, 343–353.
- Reyes-Morel, P. E., Cherng, J.-S. and Chen, I.-W., Transformation plasticity of CeO<sub>2</sub>-stabilized tetragonal zirconia polycrystals: II. Pseudoelasticity and shape memory effect. *J. Am. Ceram. Soc.*, 1988, **71**, 648–657.
- Yu, S. and Shetty, D. K., Transformation zone shape, size, and crack-growth-resistance (R-curve) behaviour of ceria-partially-stabilized zirconia polycrystals. *J. Am. Ceram. Soc.*, 1989, **72**, 921–928.
- Sun, Q., Hwang, K. C. and Yu, S. W., A micromechanics constitutive model of transformation plasticity with shear and dilatation effect. *J. Mech. Phys. Sol.*, 1991, **39**, 507–524.
- Stump, D. M., The role of shear stresses and shear strains in transformation toughening. *Phil Mag A*, 1991, **64**, 879–902.
- Stump, D. M., Autocatalysis: the self-induced growth of martensitic phase transformations in ceramics. *Acta Metall. Mater.*, 1994, **42**, 3027–3033.
- Muddle, B. C. and Hannink, R. J. H., Crystallography of the tetragonal to monoclinic transformation in MgO-partially-stabilized zirconia. *J. Am. Ceram. Soc.*, 1986, **69**, 547–555.
- Mori, T. and Tanaka, K., Average stress in matrix and average elastic energy of materials with misfitting inclusions. *Acta Metall.*, 1973, **21**, 571–574.
- Chiu, Y. P., On the stress field due to initial strains in a cuboid surrounded by an infinite elastic space. *J. Appl. Mech.*, 1977, **44**, 587–590.
- Mura, T. and Cheng, P. C., The elastic field outside an ellipsoidal inclusion. *J. Appl. Mech.*, 1977, **44**, 591–594.
- Schmauder, S. and Schubert, H., Significance of internal stresses for the martensitic transformation in yttria-stabilized tetragonal zirconia polycrystals during degradation. *J. Am. Ceram. Soc.*, 1986, **69**, 534–540.
- Lambropoulos, J. C., Shear, shape and orientation effects in transformation toughening. *Int. J. Sol. Struct.*, 1986, **22**, 1083–1106.
- Wenfang, L., Jilong, M. and Shanyi, D., The stiffness and strength of transformation toughening ceramics with misoriented microcracks. *J. Mat. Sci.*, 1994, **29**, 4252–4255.
- Wenfang, L., Jilong, M. and Shanyi, D., Transformation criterion of phase transformation toughening ceramics with misoriented microcracks. *J. Mat. Sci.*, 1997, **32**, 4149–4152.
- Rauchs, G., Fett, T., Munz, D., Oberacker, R., Tetragonal-to-monoclinic phase transformation in CeO<sub>2</sub>-stabilized zirconia under uniaxial loading. *J. Eur. Ceram. Soc.*, 2001, **21**, 2229–2241.
- Timoshenko, S. P., Goodier, J. N., Theory of elasticity. McGraw-Hill, 1970.
- Rauchs, G., *An Investigation on the Tetragonal-monoclinic Phase Transformation in CeO<sub>2</sub>-stabilized Zirconia under Multiaxial Loading* (in German). Thesis, University of Karlsruhe, 1998, Karlsruhe, Germany.
- Rauchs, G., Munz, D., Fett, T., Oberacker, R., An investigation on the critical phase transformation stresses of 9 Ce-TZP ceramics under multiaxial loading. Proceedings 9th Cimtec 1998, Part A, p. 633–40.